U.P.B. Sci. Bull., Series C, Vol. 80, Iss. 4, 2018 ISSN 2286-3540

DISTRIBUTION LINE MODEL FOR SINGLE-PHASE-TO-GROUND FAULT ANALYSIS IN DISTRIBUTION POWER SYSTEMS

Jinrui TANG[1], Jiaqi WANG[2], Chen YANG[3], Bowen LIU[4]

Zero-mode transient fault currents are widely used for faulty feeder identification under single-phase-to-ground fault in neutral non-effectively grounded distribution systems (NGDSs). Traditional distribution line model is usually constructed by single π line model, single capacitance or single T distribution line model. To evaluate the transient simulation effectiveness of the distribution models, magnitude-frequency and phase-frequency characteristics are analyzed for the common distribution line models, and sequence parameters of corresponding distribution line model are analyzed under Karrenbauer transformation matrix. The analysis and simulation results show that low pass filter should be installed to filter out the part of signal outside the first capacitive frequency band, which is calculated by the actual distributed parameter model, and parameter calculation method for traditional chain-shaped loop circuit of three-phase line model can also be used for the model presented in this paper.

Keywords: distribution network; single phase-to-ground fault; distribution line model; faulty feeder identification; zero-mode transient current

1. Introduction

In neutral non-effectively grounded distribution systems (NGDSs), digital and physical simulation techniques are usually used to obtain zero-mode transient fault currents in different feeders when single-phase-to-ground fault occurs [1-3]. And then the magnitude and phase characteristics of the transient simulation signals are analyzed by wavelet transformation or Hilbert transformation to present new method for single-phase-to-ground faulty feeder identification [4-6].

In the constructed NGDSs simulation models, distribution line models are mainly divided into two categories: 1) treat the distribution line as a single-to-ground capacitance [7-10], which is mainly used to simulate the zero-mode equivalent network. It is simple to realize the simulation and physical distribution line model using this method and can meet the demand of verifying faulty feeder identification methods based on steady-state reactive currents and voltages. But its

[1] Wuhan University of Technology, China, E-mail: tangjinrui@whut.edu.cn
[2] Wuhan University of Technology, China, E-mail: 532851165@qq.com
[3] Wuhan Electric Power Technical College, China
[4] Wuhan University of Technology, China

simulation accuracy is not high because the series impedance of the distribution line has been ignored in this method. 2) apply traditional π-type equivalent transmission line model into distribution line modeling work. Usually single π line model is used to represent the distribution line due to its short length [11-14]. This method has high simulation accuracy in steady-state analysis because the self-impedance of the distribution line and its positive-sequence, negative-sequence and zero-sequence network are completely considered in the modeling. But faulty feeder identification based on transient components are the main measures in the single-phase-to-ground fault [4-6,9,13-15], and then the applicability of single π line model used for simulation within thousands of hertz should be discussed carefully.

In fact, magnitude and phase of the actual distribution line with distribution parameter vary with frequency. For the single capacitance, single π and single T line models mentioned above, to ensure that the simulation results can be used to verify the effectiveness of the presented faulty feeder identification methods, steady-state and transient response characteristics of the distribution line models should be analyzed, and their restricted ranges should be defined.

Therefore, the magnitude-frequency and phase-frequency characteristics of each distribution line model are analyzed, as well as the error in the first capacitive frequency band, which is calculated by the distributed parameter line model. Based on this, the parameter calculation method of chain-shaped loop circuit of three-phase distribution line model is discussed. The research results can be used to construct a proper distribution line model to study and verify the single-phase-to-ground fault detection and faulty feeder identification based on steady-state and transient signals.

2. Magnitude-frequency and phase-frequency characteristics of distribution line model

2.1 Equivalent input impedance of distribution line model

Once a single-phase-to-ground fault occurs, the fault current and zero-sequence currents of each feeder are mainly determined by the zero-sequence network in NGDSs. And the steady-state and transient response characteristics of the zero-sequence network are mainly influenced by the distribution line.

In the zero-sequence network corresponding to a single-phase-to-ground fault in NGDSs, the end of the distribution line is at the condition of open circuit. Assuming the terminal open-circuit voltage equals $\dot{U}_2$, the voltage $\dot{U}_{oc}$ and current $\dot{I}_{oc}$ at the front node *x* from the terminal node can be derived by

$$\dot{U}_{oc} = \dot{U}_2 \cosh(\gamma x) \tag{1}$$

$$\dot{I}_{oc} = \frac{\dot{U}_2}{Z_c}\sinh(\gamma x) \tag{2}$$

where $Z_c = \sqrt{\dfrac{R_0 + j\omega L_0}{j\omega C_0}}$, which represents the characteristic impedance of the distribution line, R_0, L_0 and C_0 represent the series resistance, series inductance and shunt capacitance of the distribution line per unit, and ω equals the angular frequency.

So, the equivalent input impedance of the distribution line with distributed parameters at the initial node is

$$\dot{Z}_{oc} = \frac{\dot{U}_{oc}}{\dot{I}_{oc}} = Z_c\frac{\cosh(\gamma x)}{\sinh(\gamma x)} \tag{3}$$

where $\gamma = \sqrt{(R + j\omega L_0)j\omega C_0}$, which represents the propagation coefficient of the distribution line.

For the single capacitance model, the equivalent input impedance at the initial node is

$$Z^{(1)}{}_{oc}(\omega) = -j\frac{1}{\omega C_0 x} \tag{4}$$

For the single π model, the equivalent input impedance at the initial node with an open-circuit terminal node is

$$Z^{(2)}{}_{oc}(\omega) = \frac{\left(R_0 x + j\omega L_0 x - j\dfrac{2}{\omega C_0 x}\right)\times(-j\dfrac{2}{\omega C_0 x})}{R_0 x + j\omega L_0 x - j\dfrac{4}{\omega C_0 x}} \tag{5}$$

For the single *T* model, the equivalent input impedance at the initial node with an open-circuit terminal node is

$$Z^{(3)}{}_{oc}(\omega) = R_0\frac{x}{2} + j\omega L_0\frac{x}{2} - j\frac{1}{\omega C_0 x} \tag{6}$$

The equivalent input impedances of different distribution line models with open-circuit terminal node, which include single capacitance, single π and single T models, are given in equations (3), (4), (5) and (6) separately.

2.2 Magnitude-frequency and phase-frequency characteristics of each distribution line model

In this paper, typical parameters of distribution overhead lines and cables shown in Table 1 is used to analyze the magnitude-frequency and phase-frequency characteristics of each distribution line model [16]. The difference in the equivalent input impedance is calculated for x=2 km, 5km, 10 km, and 20 km, and some results are shown in Figs. 1-4.

To evaluate the difference in the phase of equivalent input impedance among single capacitance model, single π model, single T model, and distributed parameter model under the steady-state and transient response, the upper limit value f_m of the first capacitive frequency band is used to represent the diversity, which means the frequency corresponding to the initial conversion of the phase varies from -90° to 90°.

To evaluate the difference in the magnitude of equivalent input impedance for each distribution line model under the steady-state and transient response, the magnitude difference coefficient E_z is used to state the diversity, which should be calculated by the following equation (7)

$$E_z = \sum_{f=f_1}^{f_2} (E_{i,f} - E_{s,f})\Delta f \qquad (7)$$

where $E_{i,f}$ denotes the magnitude of the input impedance corresponding to model *i* at frequency *f*, and $E_{s,f}$ denotes the magnitude of input impedance corresponding to the distributed parameter line model at frequency *f*; Δf denotes the frequency calculation step used in the analysis; f_1 and f_2 are used to represent the lower and upper frequency limits of the analyzed frequency band respectively.

According to the typical single-phase-to-ground faulty feeder identification methods based on transient signals presented in literatures [4-6,9,13-15, 17-18], f_1 could be set as 50 Hz, and f_2 could be set as min. (5000 Hz, f_m).

From Figs. 1-4, it could be derived that there is large difference in the phase of the input impedance between single capacitance model and distributed parameter model. The phase corresponding to the single capacitance model always equals -90°, and the phase corresponding to the distributed parameter model varies periodically from +90° to -90° or on the contrary.

Table 1

Typical sequence parameters of distribution overhead lines and cables

	Positive			**Negative**			**Zero**		
	R [Ω/km]	***L*** [mH/km]	***C*** [μF/km]	***R*** [Ω/km]	***L*** [mH/km]	***C*** [μF/km]	***R*** [Ω/km]	***L*** [mH/km]	***C*** [μF/km]
Distribution overhead line	0.096	1.22	0.011	0.096	1.22	0.011	0.23	3.66	0.007
Distribution cable	0.11	0.52	0.29	0.11	0.52	0.29	0.34	1.54	0.19

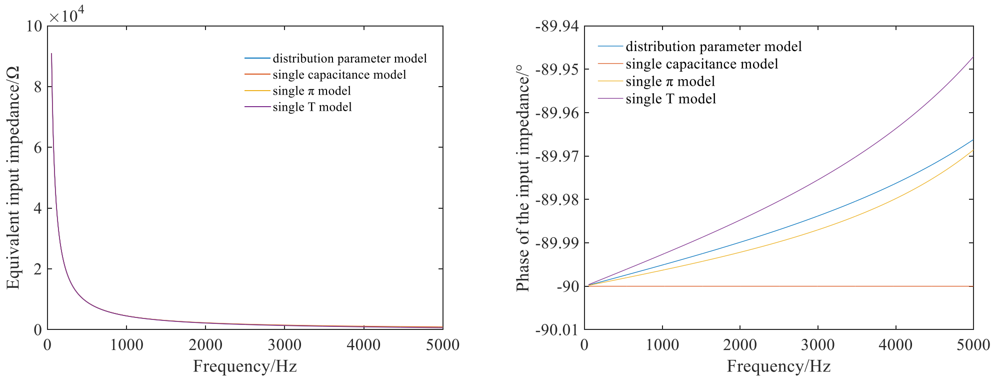

(a) magnitude-frequency characteristic; (b) phase-frequency characteristic

Fig. 1. Curves between parameter and frequency for distribution overhead line with length of 5km

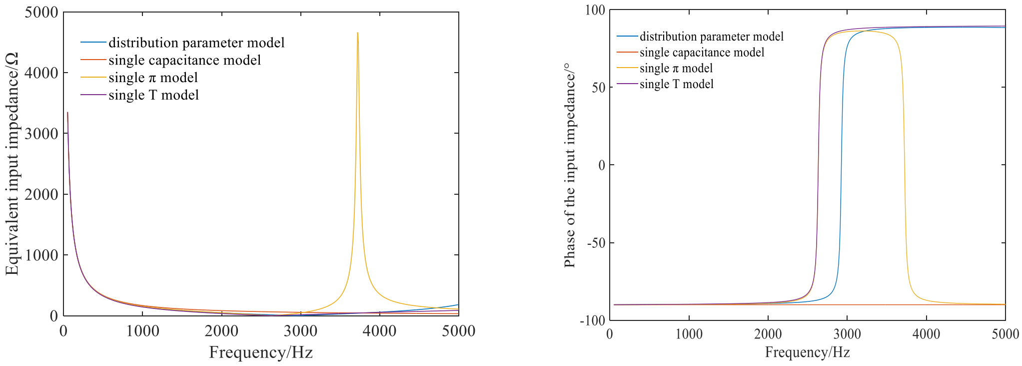

(a) magnitude-frequency characteristic; (b) phase-frequency characteristic

Fig. 2. Curves between parameter and frequency for distribution cable with length of 5km

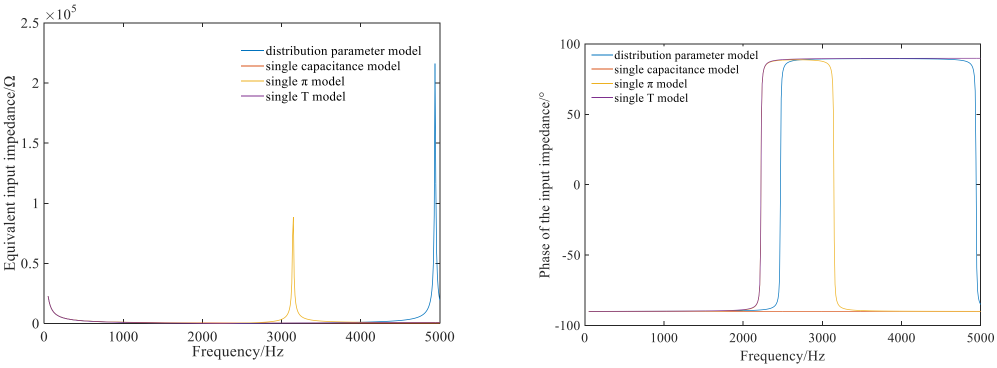

(a) magnitude-frequency characteristic; (b) phase-frequency characteristic

Fig.3. Curves between parameter and frequency for distribution overhead line with length of 20km

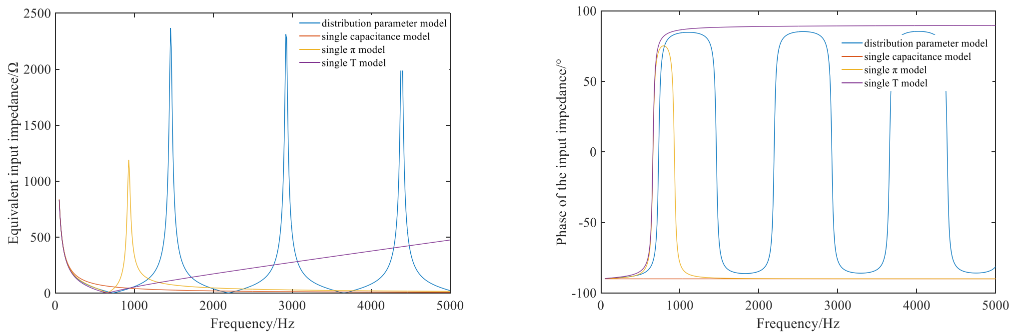

(a) magnitude-frequency characteristic; (b) phase-frequency characteristic

Fig. 4. Curves between parameter and frequency for distribution cable with length of 20km

To further clarify the differences between the simplified distribution line model and distributed parameter model under different lengths, the differences are detailed shown in Table 2. And the following results can be derived: 1) The magnitude of the input impedance for the single capacitance model nearly equals the magnitudes of other distribution line models in the first capacitive frequency band. 2) Whether it is an overhead line or a cable, the single π model and single T model can accurately simulate phase-frequency and magnitude-frequency characteristics of the distribution line. For the overhead line and cable with a length of 20 km, the corresponding upper limit values of the first capacitive frequency band of the distributed parameter line are 2470 Hz and 730 Hz, respectively, while the values for the single π and single T model are 2220 Hz and 660 Hz, respectively. So, the errors are 250 Hz and 70 Hz, respectively, which means that the single π and single T model could meet the simulation demand of single-phase-to-ground fault detection and identification.

Table 2

Input impedance between the lumped parameter modes and distributing parameter model

Length [km]	**Type**	**Difference in magnitude [Ω·Hz]**			**Difference in Phase [Hz]**			
		Single capacitance model	**Single π model**	**Single T model**	**Single capacitance model**	**Single π model**	**Single T model**	**Distribution parameters model**
2	Overhead line	3.8×10^3	3.8×10^3	3.8×10^3	>5000	>5000	>5000	>5000
	cable	1.6×10^3	1.6×10^3	1.6×10^3	>5000	>5000	>5000	>5000
5	Overhead line	9.5×10^3	9.5×10^3	9.5×10^3	>5000	>5000	>5000	>5000
	cable	2.3×10^3	2.3×10^3	2.3×10^3	>5000	2600	2600	2900
10	Overhead line	1.9×10^4	1.9×10^4	1.9×10^4	>5000	4450	4450	4900
	cable	2.3×10^3	2.3×10^3	2.3×10^3	>5000	1320	1320	1460

20	Overhead line	1.9×10^4	1.9×10^4	1.9×10^4	>5000	2220	2220	2470
	cable	2.0×10^3	2.0×10^3	2.0×10^3	>5000	660	660	730

Annotation: magnitude difference refers to the sum of the difference in magnitude within the interval from the industrial frequency to the upper limit of the capacitive frequency band, and the phase difference refers to the comparison of the upper limit frequency of the first capacitive frequency band.

Therefore, a low-pass filter should be added to filter out the signal outside the first capacitive frequency band when single capacitance, single π or single T distribution model is used to construct the distribution power system. The parameters of the low-pass filter can be identified with reference to the upper limit value of the first capacitive frequency band.

3. Parameter calculation method for three-phase distribution line model

3.1 Chain-shaped loop circuit model of three-phase distribution line

Since the medium-voltage power distribution line consists of three-phase AC lines, each phase has its self-impedance, and mutual inductance and capacitance also exist between the phase and phase, as well as between the phase and the earth. When lumped parameters are used to simulate the distributed parameter line, the mutual connection should be considered. At present, chain-shaped loop circuit model is usually used to construct the three-phase AC lines, which is shown in Fig. 5.

In Fig. 5, L_1, R_1, C_1, and l represent the positive-sequence self-inductance, positive-sequence resistance, positive-sequence capacitance, and distribution line length, respectively; C_N, L_N and R_N should be obtained by equations (8) and (9) [19]. That is, C_N, L_N and R_N are identified by the positive-sequence parameters and zero-sequence parameters of the distribution line to ensure that chain-shaped loop circuit model can accurately simulate the zero-sequence parameter of the actual distribution line.

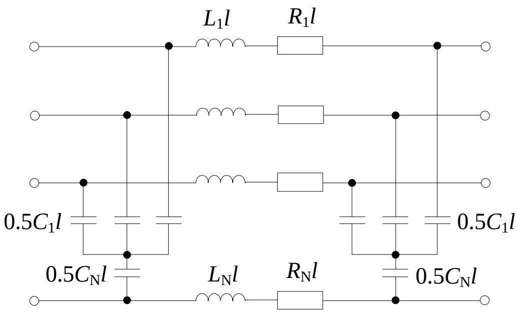

Fig. 5. Chain-shaped loop circuit of three-phase distribution line model

$$C_N = \frac{3C_1C_0}{C_1 - C_0} \tag{8}$$

$$L_N = \frac{L_0 - L_1}{3}, R_N = \frac{R_0 - R_1}{3} \tag{9}$$

where L_0, R_0, and C_0 are the zero-sequence self-inductance, zero-sequence resistance, and zero-sequence capacitance of the distribution line, respectively.

3.2 Parameter calculation for Chain-shaped loop circuit model of Distribution Line

It is important to note that the positive-sequence and zero-sequence impedances given in equations (8) and (9) are calculated from the principle of the traditional symmetric component method. But in the transient analysis, response should be analyzed under a wide frequency range from power frequency to several kilohertz. And then Karrenbauer transformation should be used to identify the parameters [20].

Taking a three-phase lossless line as an example, the voltage and current can be expressed as a function of time t and distance x, which are shown as follows

$$-\begin{bmatrix} \frac{\partial u_A}{\partial x} \\ \frac{\partial u_B}{\partial x} \\ \frac{\partial u_C}{\partial x} \end{bmatrix} = \begin{bmatrix} L_s & L_m & L_m \\ L_m & L_s & L_m \\ L_m & L_m & L_s \end{bmatrix} \begin{bmatrix} \frac{\partial i_A}{\partial t} \\ \frac{\partial i_B}{\partial t} \\ \frac{\partial i_C}{\partial t} \end{bmatrix} \tag{10}$$

$$-\begin{bmatrix} \frac{\partial i_A}{\partial x} \\ \frac{\partial i_B}{\partial x} \\ \frac{\partial i_C}{\partial x} \end{bmatrix} = \begin{bmatrix} k_s & k_m & k_m \\ k_m & k_s & k_m \\ k_m & k_m & k_s \end{bmatrix} \begin{bmatrix} \frac{\partial u_A}{\partial x} \\ \frac{\partial u_B}{\partial x} \\ \frac{\partial u_C}{\partial x} \end{bmatrix} \tag{11}$$

where k_s equals C_0+2C_m; k_m equals -C_m; L_s represents the series inductance of each phase conductor; L_m is the mutual inductance between one phase to another phase conductor; C_0 is the phase-to-ground capacitance, C_m is the phase-to-phase capacitance; x is the distance from the node to the terminal, u_A、u_B、u_C are instantaneous voltages of phase A, B and C, respectively; i_A、i_B, and i_C are instantaneous currents of phase A, B and C, respectively.

Equations (10) and (11) can be rewritten in matrix form as

$$-\frac{\partial \mathbf{u}}{\partial x} = \mathbf{L}\frac{\partial \mathbf{i}}{\partial t} \tag{12}$$

$$-\frac{\partial \mathbf{i}}{\partial x} = \mathbf{C}\frac{\partial \mathbf{u}}{\partial t} \tag{13}$$

Since there are nonzero off-diagonal elements in ***L*** and ***C*** matrix in equations (12) and (13), it is not easy to solve the equations. And then coordinate transformation should be applied to change off-diagonal elements of the coefficient matrix to zero. Both symmetric component transformation and Karrenbauer transformation can be used as the proper transformation.

For traditional symmetric component transformation, assuming

$$\mathbf{S} = \frac{\mathbf{u}}{\mathbf{u}_m} = \frac{\mathbf{i}}{\mathbf{i}_m} = \begin{bmatrix} 1 & 1 & 1 \\ 1 & a^2 & a \\ 1 & a & a^2 \end{bmatrix} \tag{14}$$

where **S** represents the transformation matrix; $\boldsymbol{u}=[u_A,u_B,u_C]^T$; $\boldsymbol{i}=[i_A,i_B,i_C]^T$; $\boldsymbol{u}_m=[u_0,u_+,u_-]^T$; $\boldsymbol{i}_m=[i_0,i_+,i_-]^T$. Among them, symbol 0, symbol + and symbol - represent zero sequence, positive sequence and negative sequence, respectively. And the variable a equals $e^{-120°}$ in the matrix.

Then equation (15) can be derived

$$\begin{cases} \dfrac{\partial^2 \mathbf{u}_m}{\partial x^2} = \mathbf{S}^{-1}\mathbf{LCS}\dfrac{\partial^2 \mathbf{u}_m}{\partial t^2} = \mathbf{D}_u \dfrac{\partial^2 \mathbf{u}_m}{\partial t^2} \\ \dfrac{\partial^2 \mathbf{i}_m}{\partial x^2} = \mathbf{S}^{-1}\mathbf{LCS}\dfrac{\partial^2 \mathbf{i}_m}{\partial t^2} = \mathbf{D}_i \dfrac{\partial^2 \mathbf{i}_m}{\partial t^2} \end{cases} \tag{15}$$

where

$$\mathbf{D}_u = \mathbf{D}_i = \mathbf{S}^{-1}\mathbf{LCS} = \\ = \begin{bmatrix} (L_s+2L_m)(K_s+2K_m) & 0 & 0 \\ 0 & (K_s-K_m)(L_s-L_m) & 0 \\ 0 & 0 & (K_s-K_m)(L_s-L_m) \end{bmatrix} \tag{16}$$

Therefore, for sequence parameters in the symmetric component transformation, the following results can be obtained: $L_0=L_s+2L_m$, $C_0=K_s+2K_m$, $L_1=L_2=L_s-L_m$, $C_1= C_2=K_s-K_m$.

For Karrenbauer transformation, assuming

$$\mathbf{S}^{(2)} = \frac{\mathbf{u}}{\mathbf{u}_m} = \frac{\mathbf{i}}{\mathbf{i}_m} = \begin{bmatrix} 1 & 1 & 1 \\ 1 & -2 & 1 \\ 1 & 1 & -2 \end{bmatrix} \tag{17}$$

Then equation (18) can also be obtained

$$\mathbf{D}_u^{(2)} = \mathbf{D}_i^{(2)} = \mathbf{S}^{(2)\text{-}1}\mathbf{LCS}^{(2)} = \begin{bmatrix} (k_s+2k_m)(L_s+2L_m) & 0 & 0 \\ 0 & (k_s-k_m)(L_s-L_m) & 0 \\ 0 & 0 & (k_s-k_m)(L_s-L_m) \end{bmatrix} \quad (18)$$

Therefore, for sequence parameters in the Karrenbauer transformation, the following results can be obtained: $L_0^{(2)}=L_s+2L_m$, $C_0^{(2)}=K_s+2K_m$, $L_1^{(2)}=L_2^{(2)}=L_s-L_m$, $C_1^{(2)}= C_2^{(2)}=K_s-K_m$.

In conclusion, for the same distribution line, the sequence parameters in the Karrenbauer transformation are the same as that in traditional symmetric component transformation. In other words, when a three-phase model of a distribution line is modeling, its traditional parameters in symmetric component transformation can directly be used to analyze the transient response.

4. Conclusions

Based on the principle of the first capacitive frequency band, distribution line model for single-phase-to-ground fault analysis in NGDSs is analyzed under steady-state and transient response. The main conclusions are as follows:

(1) The single capacitance model, single π model and single T model can all accurately simulate the magnitude-frequency characteristic of the distributed parameter line in the first capacitive frequency band. To ensure the correct estimate of the phase-frequency characteristic, a low-pass filter should be installed to filter out the part of signal outside the first capacitive frequency band, which is calculated by the actual distributed parameter model.

(2) For the three-phase distribution line model using chain-shaped loop circuit model, its traditional parameters in symmetric component transformation can directly be used to analyze the transient response, that is, the sequence parameters in the Karrenbauer transformation are the same as that in traditional symmetric component transformation.

Acknowledgement

This work was supported by the National Natural Science Foundation of China (Grant No. 51707139).

REFERENCES

[1]. *Yankan Song, Ying Chen, Shaowei Huang, et al*. Fully GPU-based electromagnetic transient simulation considering large-scale control systems for system-level studies[J]. IET Generation, Transmission& Distribution, 2017, 11(11): 2840-2851.

[2]. *Jorge Jardim, Karen Caino de Oliveira Salim, Pedro Henrique Lourenco dos Santos, et al*. *Variable* time step application on hybrid electromechanical-electromagnetic simulation[J]. IET Generation, Transmission & Distribution, 2017, 11(12): 2968-2973.

[3]. *Nagy I. Elkalashy, Matti Lehtonen, Hatem A. Darwish, et al*. Modeling and experimental verification of high impedance arcing fault in medium voltage networks[J]. IEEE Transactions on Dielectrics and Electrical Insulation, 2007, 14(2): 375-383.

[4]. *Yongduan Xue, Xiaoru Chen, Huamao Song, et al*. Resonance analysis and faulty feeder identification of high-impedance faults in a resonant grounding system[J]. IEEE Transactions on Power Delivery, 2017, 32(3): 1545-1555.

[5]. *Yuanyuan Wang, Yuhao Huang, Xiangjun Zeng, et al*. Faulty feeder detection of single phase-earth fault using grey relation degree in resonant grounding system[J]. IEEE Transactions on Power Delivery, 2017, 32(1): 55-61.

[6]. *Jinrui Tang, Xianggen Yin, Minghao Wen, et al*. Fault location in neutral non-effectively grounded distribution systems using phase current and line-to-line voltage[J]. Electric Power Components and Systems, 2014, 42(13): 1371-1385.

[7]. *Peng Wang, Baichao Chen, Cuihua Tian, et al*. A novel neutral electromagnetic hybrid flexible grounding method in distribution networks[J]. IEEE Transactions on Power Delivery, 2017, 32(3): 1350-1358.

[8]. *Wen Wang, Lingjie Yan, Xiangjun Zeng, et al.* Principle and design of a single-phase inverter-based grounding system for neutral-to-ground voltage compensation in distribution networks[J]. IEEE Transactions on Industrial Electronics, 2017, 64(2): 1204-1213.

[9]. *M.F. Abdel-Fattah, M. Lehtonen.* Transient algorithm based on earth capacitance estimation for earth-fault detection in medium-voltage networks[J]. IET Generation, Transmission & Distribution, 2012, 6(2): 161-166.

[10].*N. Kolcio, J.A. Halladay, G.D. Allen, et al.* Transient overvoltages and overcurrents on 12.47kV distribution lines: computer modeling results[J]. IEEE Transactions on Power Delivery, 1993, 8(1): 359-366.

[11].*Ye Cheng, Zhigang Liu, Ke Huang.* Transient analysis of electric arc burning at insulated rail joints in high-speed railway stations based on state-space modeling[J]. IEEE Transactions on Transportation Electrification, 2017, 3(3): 750-761.

[12].*Peng Wang, Baichao Chen, Hong Zhou, et al*. Fault location in resonant grounded network by adaptive control of neutral-to-earth complex impedance[J]. IEEE Transactions on Power Delivery, 2018, 33(2): 689-698.

[13].*Amir Farughian, Lauri Kumpulainen, Kimmo Kauhaniemi.* Review of methodologies for earth fault indication and location in compensated and unearthed MV distribution networks[J]. Electric Power Systems Research, 2018(154): 373-380.

[14].*A. Bahmanyar, S. Jamali, A. Estebsari, et al.* A comparison framework for distribution system outage and fault location methods[J]. Electric Power Systems Research, 2017(145): 19-34.

[15].*Tao Cui, Xinzhou Dong, Zhiqian Bo, et al.* Hilbert-transform-based transient/intermittent earth fault detection in noneffectively grounded distribution systems, 2011, 26(1): 143-151.

[16].*Jinrui Tang, Chen Yang, Lijun Cheng.* Analysis on zero-sequence current variation characteristic for feeders of distribution network at different residual current compensation factors[J]. Automation of Electric Power Systems, 2017, 41(13): 125-132. (in Chinese)

[17].*Hongchun Shu, Shixin Peng, Bin Li, et al.* A new approach to detect fault line in resonant earthed system using simulation after test[J]. Proceedings of the CSEE, 2008, 28(16): 59-64. (in Chinese)

[18].*Jianwen Zhao, Yongjia Liu, Jing Liang, et al*. Fault line selection based on improved FastICA and Romanovsky guidelines[J]. Proceedings of the CSEE, 2016, 36(19): 5209-5218.

[19].*Panos C. Kotsampopoulos, Vasilis A. Kleftakis, Nikos D*. Hatziargyriou. Laboratory education of modern power systems using PHIL simulation[J]. IEEE Transactions on Power Systems, 2017, 32(5): 3992-4001.

[20].*Shicong Ma, Bingyin Xu, Houlei Gao, et al*. An improved differential equation method for earth fault location in non-effectively earthed system[C]. 10th IET International Conference on Developments in Power System Protection, Manchester, UK, 2010.